Connection between Noise-Induced Symmetry Breaking and an Information-Decoding Function for Intracellular Networks

Tetsuya J. Kobayashi*

Institute of Industrial Science, The University of Tokyo, 4-6-1 Komaba Meguro-ku, Tokyo 153-8505, Japan

(Received 15 February 2011; published 2 June 2011)

The biological function of noise-induced symmetry breaking (NISB) is still unclear even though it may potentially occur in noisy intracellular systems. In this work, I demonstrate that information decoding from a noisy signal is a potential biological function of NISB by revealing that NISB naturally emerges from an optimal information-decoding dynamics and that several intracellular networks can be identified with the information-decoding dynamics. I also propose a mean first passage time profile as a way to experimentally identify NISB.

DOI: 10.1103/PhysRevLett.106.228101 PACS numbers: 87.18.Tt, 05.40.Ca, 87.10.Mn, 87.18.Vf

Intracellular systems are full of a variety of dynamical phenomena. Unlike nonbiological systems, however, most of intracellular dynamics is considered to have its own biological functions that contribute to the fitness of a cell. Deterministic symmetry breaking (SB) and the associated bistability, for example, can have biological functions to realize all-or-none responses in differentiation and polarity formation, irreversibility in apoptosis and the cell cycle, and history-dependent memory in development and epigenetics [1]. Thus, for a comprehensive understanding of intracellular dynamics, it is indispensable to reveal not only the mechanism that generates the dynamics but also the biological function of the dynamics.

However, we still lack the knowledge on potential functionalities of some intracellular dynamics in spite of their biological relevance and importance. An example is noise-induced symmetry breaking (NISB) in which noise induces the emergence of a bimodal distribution even though no deterministic SB occurs under the noiseless condition [2]. Its presence has recently been suggested more specifically in relation to several intracellular phenomena such as the autocatalytic cycles [3], the phosphorylation-dephosphorylation cycle [4], an endocytic pathway of Rab5 GTPase [5], *T*-cell response [6], and spontaneous polarization in budding yeast [7]. Nonetheless, the NISB and its related dynamics still do not attract sufficient attention because its particular biological functions remain unclear. Furthermore, the experimental challenge of identifying the NISB is also hampered by the lack of theoretical criteria to distinguish between deterministic and NISBs even though bimodal distributions have been observed experimentally in several intracellular systems [8].

In this work, I reveal that the decoding of information from a noisy signal can be a significant biological function of NISB in various intracellular networks and propose an experimental procedure to identify the NISB. Toward this purpose, I first show that an intracellular network that can decode (extract) relevant information from a noisy signal naturally poses an ability to show NISB.

The following autophosphorylation and autodephosphorylation cycle (aPadP cycle) was clarified in Ref. [9] as an intracellular network that is approximately equivalent to an optimal dynamics to decode the state of environment x_t from noisy receptor signal $S(t)$ [Figs. 1(a) and 1(b)]:

$$\frac{dZ}{dt} = F(Z, S(t))\tilde{Z} - G(\tilde{Z})Z + r_{\mathrm{on}}\tilde{Z} - r_{\mathrm{off}}Z, \qquad (1)$$

where $F(Z, S) := \lambda_r N_0 SZ$, $G(\tilde{Z}) := \lambda_d N_0 \tilde{Z}$, $\lambda_r = \log(\lambda_{\mathrm{on}}/\lambda_{\mathrm{off}})$, and $\lambda_d = \lambda_{\mathrm{on}} - \lambda_{\mathrm{off}}$ [Fig. 1(a)]. $Z \in [0, 1]$ and $\tilde{Z} := 1 - Z$ are the ratios of phosphorylated and unphosphorylated molecules, respectively. $F(Z, S)$ and $G(\tilde{Z})$ represent rate constants of the autoregulatory phosphorylation and dephosphorylation, respectively. $r_{\mathrm{on}}\tilde{Z}$ and $r_{\mathrm{off}}Z$ are, respectively, leaky phosphorylation and dephosphorylation reactions that occur spontaneously. $x_t \in \{0, 1\}$ is a

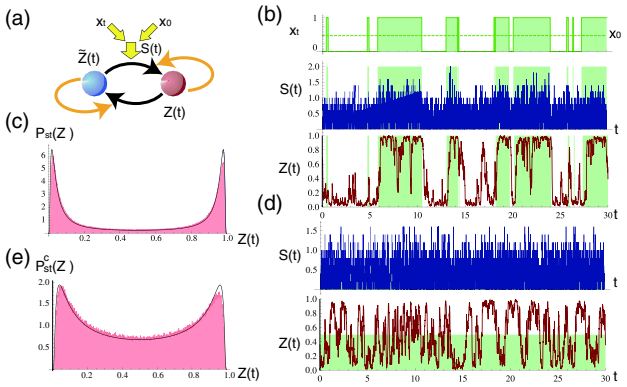

FIG. 1 (color online). Schematic diagram of the aPadP cycle (a) and its stationary distributions driven by changing input x_t (b) and constant input x_0 (d). The red and black curves are Monte Carlo simulations of Eq. (1) and the analytic solution of Eq. (2), respectively. The time series of the input x_t (green curves and regions), noisy signal $S(t)$ (blue curves), and response of the aPadP cycle $Z(t)$ (red curves) for changing input x_t (c) and a constant input x_0 (e). In all of the panels, $\lambda_{\mathrm{on}} = 0.47$, $\lambda_{\mathrm{off}} = 0.33$, $r_{\mathrm{on}} = r_{\mathrm{off}} = 1/2$, $\tau = 0.01$, and $N_0 = 500$.

binary environmental state that randomly changes between the on state (denoted by 1) and the off state (denoted by 0) over time by following a time-continuous two-state Markov process whose instantaneous rates of transition from $0 \to 1$ and $1 \to 0$ are $r_{\rm on}$ and $r_{\rm off}$, respectively. $S(t)$ is a noisy observation of x_t by receptors of the cell and is modeled by a counting process $N_P(t)$ as $S(t) = [N_P(t) - N_P(t-\tau)]/(\tau N_0)$. In this interpretation, $N_P(t)$ represents the total counts of receptor activations until t and thus follows $\mathbb{P}\{[N_P(t') - N_P(t)] = n\} = e^{-\lambda(t';t)}\lambda(t';t)^n/(n!)$, where $\lambda(t';t) := \int_t^{t'} N_0\lambda(t)dt$ and $\lambda(t) = [\lambda_{\rm on}x_t + \lambda_{\rm off}(1 - x_t)]$. Here, N_0 and $\lambda(t)$ are the total number of receptors and the rate of activation of each receptor at t, respectively. In addition, because τ is the time required for the inactivation of the receptor, $N_P(t-\tau)$ represents the total counts of inactivations until t. Thus, $N(t) := N_P(t) - N_P(t-\tau)$ corresponds to the number of active receptors at t [9] (see also [10]).

As demonstrated in Fig. 1(b), the aPadP cycle can decode (extract) the information of x_t from extremely noisy $S(t)$, which is a crucial function for a cell to survive in an unpredictably changing environment with its noisy components. Because $Z(t)$ decodes x_t, which switches between 0 and 1, its stationary distribution $\mathbb{P}_{st}(Z)$ can be bimodal [Fig. 1(c)]. However, even if the aPadP cycle is driven not by the changing x_t but by a constant x_0 with intermediate value $x_0 \approx 1/2$, it still will have an ability to break its symmetry spontaneously by generating a bimodal stationary distribution $\mathbb{P}^c_{st}(Z)$ [Figs. 1(d) and 1(e)].

To further clarify dynamical properties of the x_t-driven and spontaneous SBs, I derive the following Gaussian approximation of Eq. (1) (see [10] for a derivation):

$$dZ = [\mu(t)Z\tilde{Z} + \gamma_{\rm on}\tilde{Z} - \gamma_{\rm off}Z]dt + \sigma Z\tilde{Z} \circ dW_t, \quad (2)$$

where $\nu := \lambda_d^2 N_0/(2\lambda_{\rm off})$, $r_t = r_{\rm on} + r_{\rm off}$, $\sigma := \sqrt{2\nu/r_t}$, $\mu(t) := [\alpha(t) - 1/2]\sigma^2$, $\gamma_{\rm on} := r_{\rm on}/r_t$, and $\gamma_{\rm off} := r_{\rm off}/r_t$. $\circ$ represents the Stratonovich integral, and the time scale of the system is rescaled by r_t. In Eq. (2), $S_g(t) := \mu(t) + \sigma \circ dW_t$ is the Gaussian counterpart of the noisy signal $S(t)$ in Eq. (1). The corresponding Fokker-Planck equations for $\alpha(t) = x_t$ [$\mu(t) = \sigma^2(x_t - 1/2)$] and for $\alpha(t) = x_0$ [$\mu_0 = \sigma^2(x_0 - 1/2)$] are $d\mathbb{P}(Z)/dt = -\partial[L(Z)\mathbb{P}(Z)]/(\partial Z) + (\sigma/2)\partial^2[Z\tilde{Z}\mathbb{P}(Z)]/(\partial Z^2)$ and $d\mathbb{P}(Z)/dt = -\partial\{[\mu_0\tilde{Z}Z + L(\tilde{Z})]\mathbb{P}(Z)\}/(\partial Z) + (\sigma/2)\partial[Z\tilde{Z}\partial\mathbb{P}(Z)/(\partial Z)]/(\partial Z)$, respectively (see [10]). Here, $L(Z) := (\gamma_{\rm on}\tilde{Z} - \gamma_{\rm off}Z)$. Their stationary distribution can be obtained analytically as in [10]. If $\gamma_{\rm on} = \gamma_{\rm off} = 1/2$ holds, as in Fig. 1, the analytical expressions can be further simplified as $\mathbb{P}_{st}(Z) = C\exp\{-[1/(Z\tilde{Z})]/\sigma^2\}/(Z\tilde{Z})^2$ and $\mathbb{P}^c_{st}(Z) = C'\exp\{-[1/(Z\tilde{Z}) + 2\mu_0\ln(\tilde{Z}/Z)]/\sigma^2\}/Z\tilde{Z}$, where C and C' are normalization constants. The analytical expression shows that $\mathbb{P}_{st}(Z)$ becomes bimodal when $\sigma > \sqrt{2}$, and the peak positions satisfy $H(Z_{st};\sigma) := 2\sigma^2 Z_{st}^2 - 2\sigma^2 Z_{st} + 1 = 0$ [Fig. 2(a)]. Because $\sigma^2 \propto \nu$ and ν corresponds to the instantaneous information gain obtained from $S(t)$ on x_t (see [10]), $\sigma > \sqrt{2}$ indicates that x_t-driven SB appears only when $S(t)$ contains sufficient information on x_t [9]. Therefore, x_t-induced SB reflects the efficiency of information decoding by Z. Similarly, $\mathbb{P}^c_{st}(Z)$ also has two peaks when $|\mu_0|$ is close to 0 and σ is sufficiently large. In particular, when $\mu_0 = 0$ (which is equivalent to $x_0 = 1/2$), $\sigma > 2$ is the condition for the bimodality. Furthermore, the two peaks satisfy $H^c(Z_{st};\sigma) := \sigma^2 Z_{st}^2 - \sigma^2 Z_{st} + 1 = 0$ [Fig. 2(a)], which coincides with $H(Z_{st};\sigma)$ by scaling σ as $H(Z_{st};\sigma) = H^c(Z_{st};\sqrt{2}\sigma)$. These results indicate that the information-decoding dynamics by the aPadP cycle accompanies spontaneous SB under the intermediate constant input $x_0 = 1/2$, and that its information-decoding function can be inferred from the related spontaneous SB (see [10] for $\gamma_{\rm on} \neq \gamma_{\rm off}$).

At first sight, the spontaneous SB of $\mathbb{P}^c_{st}(Z)$ appears to be deterministic because the positive regulations of the autophosphorylation and autodephosphorylation seem to create a deterministically bistable potential [Fig. 1(a)]. However, Eq. (2) shows that it only has a single stationary state deterministically for all constant μ_0 because its deterministic potential $V(Z;\mu) := Z[\mu Z^2/3 + (1-\mu)Z/2 - \gamma_{\rm on}] + C''(\mu)$ has only one minimum within $0 \le Z \le 1$. Thus, the deterministic potential alone never generates the spontaneous SB. Rather, it is induced by noise. Because the signal $S_g(t)$ that contains both the input $\mu(t)$ and the noise dW_t is multiplied by $Z\tilde{Z}$, the system has a slow time scale near $Z = 1$ or $Z = 0$, whereas it has a fast time scale near $Z = 1/2$. This nonhomogeneity of the time scale, especially for the noise, creates the bimodality because the system tends to spend more time near $Z = 1$ and $Z = 0$. In this mechanism, stronger noise can induce spontaneous SB [Fig. 2(b)], in sharp contrast to deterministic spontaneous SB, where noise just blurs the deterministic bistable structure [Fig. S2(a) in [10]]. This NISB has been known mathematically as a pure noise-induced transition [2] and is equivalent to the noise-induced phenomena reported previously for various intracellular systems [3–7,11]. However, its biological function has been unclear both theoretically and experimentally. This result reveals that NISB under constant input x_0 and the information-decoding function under changing input x_t are tightly connected to each other. This connection in turn strongly suggests that an intracellular network that can show NISB

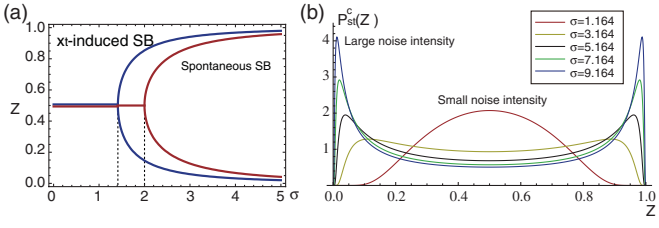

FIG. 2 (color). (a) Peak positions of $\mathbb{P}_{st}(Z)$ (blue curve) and $\mathbb{P}^c_{st}(Z)$ (red curve) as functions of σ, where $\mu = 0$ and $\gamma_{\rm on} = \gamma_{\rm off} = 1/2$. (b) The stationary distributions of Eq. (2) for different values of σ, where $\mu = 0$ and $\gamma_{\rm on} = \gamma_{\rm off} = 1/2$.

may have a hidden function to decode information even though its network structure is seemingly different from that of the aPadP cycle. Next, I demonstrate the equivalence of the aPadP cycle with a modified version of a T-cell response model reported to have noise-induced SB [6].

T-cell response is modeled by a simplified dueling reaction between agonistic and antagonistic signals $S_P(t)$ and $S_N(t)$, respectively [Fig. 3(a)]. The receptors not induced, induced by $S_P(t)$, and induced by $S_N(t)$ are designated here as A, A_P, and A_N, respectively. While positive feedback regulation is assumed only for the inductions by the agonist in [6], I include both positive regulative and nonregulative terms for both inductions for generality as

$$\begin{aligned} \frac{dA}{dt} &= \upsilon_A - [S_P(t)A_P + S_N(t)A_N]A - (k_P + k_N)A, \\ \frac{dA_o}{dt} &= S_o(t)A_oA + k_oA - dA_o, \qquad o \in \{P, N\}. \end{aligned} \tag{3}$$

Let $A_{PN} := A_P + A_N$, $Z := A_P/A_{PN}$, and $\tilde{Z} := A_N/A_{PN}$. If $|S_P(t) - S_N(t)| \ll S_P(t), S_N(t)$, then we can derive $dZ/dt = A[S_P(t) - S_N(t)]Z\tilde{Z} + a[k_P\tilde{Z} - k_NZ]$, where $a = A/A_{PN}$ is approximately constant (see [10] for the details). If we identify $AS_P(t)$, $AS_N(t)$, ak_P, and ak_N with $N_0\lambda_rS(t)$, $N_0\lambda_d$, r_{on}, and r_{off} in Eq. (1), respectively, then this equation is equivalent to Eq. (1), indicating that the dueling reaction of the T-cell response has the potential to detect (decode) a small change in $S_P(t)$ due to the agonist even with erroneous signals in $S_P(t)$ and $S_N(t)$. Similar results can also be obtained for a polarity formation [Fig. S2(b) in [10]], a zero-order phosphorylation-dephosphorylation cycle, and population dynamics (see [10]), although not all NISBs are equivalent to the decoding dynamics. This suggests that the connection of NISB and its information-decoding function may be also found in various other networks.

To further test the validity of this connection, the experimental identification of the NISB will be crucial. While the emergence of bimodal distributions has been observed experimentally in several cellular phenomena [8], a bimodal distribution alone is not sufficient to distinguish the NISB from the deterministic SB. For example, a stationary distribution that is exactly the same as $\mathbb{P}^c_{st}(\mathbb{P})$ can also be realized by a double-well potential $V_{ef}(Z)$, with additive noise as

$$dZ = -\upsilon\frac{dV_{ef}(Z)}{dZ}dt + \sqrt{\upsilon}\sigma \circ dW_t, \tag{4}$$

where $V_{\text{ef}}(Z) = [(\gamma_{\text{on}} - \gamma_d Z)/(Z\tilde{Z}) + (\mu + \gamma_d)\ln(\tilde{Z}/Z)] - (\sigma^2/2)\ln Z\tilde{Z}$. υ is a time constant that cannot be determined solely from $\mathbb{P}^c_{st}(Z)$. While the response of the distribution to the change in noise intensity may discriminate between the two SBs [Fig. 2(b) and Fig. S2(a) in [10]], it is still difficult to experimentally change just the noise intensity because the deterministic dynamics and noise usually share some parameters in intracellular networks. Experimentally feasible is a way to exploit the dynamic information of a system without external perturbations and mutations such as the trajectories under constant input. While the trajectories generated by two SBs seem to have little difference (Fig. S3 in [10]), they are qualitatively distinguished by their mean first passage time (mFPT) profiles $T(Z; Z_L)$, defined as the average time, starting from the left peak Z_L to reach Z for the first time, where $Z_L \le Z \le Z_R$. Figure 3(b) shows that the shape of the mFPT profile for the deterministic bimodal distribution, $T_{ef}(Z; Z_L)$, is sigmoidal, whereas that of the noise-induced one, $T_{\text{ni}}(Z; Z_L)$, is antisigmoidal.

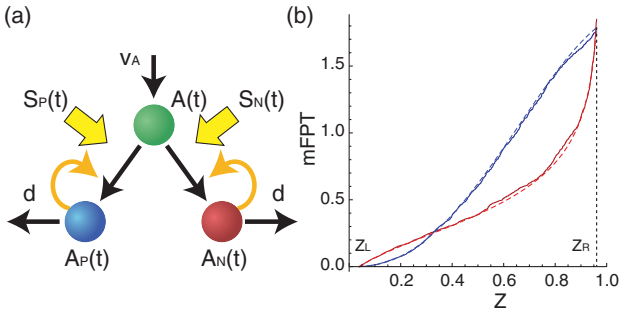

FIG. 3 (color). (a) Schematic diagram of the T-cell response model. (b) The mFPT of Eq. (2), T_{ni} (red curve), and Eq. (4), T_{ef} (blue curve). The solid and dashed curves are obtained by Monte Carlo simulations with 1000 samples and numerical integration of the analytical representation of the mFPT, respectively. All the parameters other than υ are the same as those in Fig. 1(e). υ is determined so that the mFPT of Eq. (3) coincides with that of Eq. (2) at right peak Z_R.

This qualitative difference is owing to the difference between their mechanisms to generate SB. The sigmoidal shape appears in the deterministic case because it takes the longest time to cross the potential barrier between two wells. In the noise-induced case, by contrast, its state resides near the two peaks but quickly goes through the bottom of the stationary distribution because of the nonhomogeneity in the time scale, which results in the antisigmoidal shape of the mFPT profile. Because single-cell time-lapse measurement is now a popular imaging technique and the qualitative difference in the shape of profiles is a robust measure to distinguish underlying mechanisms [12], the mFPT profile can serve as a criterion for experimentally identifying NISB and its associated function to decode information (see also [10]).

As the mFPT profile clarified, the state-dependent nonhomogeneous time scale is essential not only to the generation but also to the dynamical properties of NISB. Its role can be illustrated more clearly by changing the variable of Eq. (2) from Z to $\theta = \log Z/(1 - Z)$ as $d\theta = [\mu(t)dt + \sigma \circ dW_t] - (1 + e^{\theta})(\gamma_{\text{off}} - \gamma_{\text{on}}e^{-\theta})dt$. This coordinate transformation converts the equation for Z with the multiplicative noise into an equation for θ with an additive noise, meaning that the nonhomogeneous time scale is resolved in the θ coordinate. The deterministic potential for the dynamics of θ is $V(\mu, \theta) := -\theta\mu + V_f(\theta)$,

where $V_f(\theta) := -\theta\gamma_d + \gamma_{\mathrm{off}}e^{\theta} + \gamma_{\mathrm{on}}e^{-\theta}$ and has only one minimum for constant $\mu(t) = \mu_0$ at $\theta_{st} = \log\{[\mu_0 + \gamma_d + \sqrt{(\mu_0 + \gamma_d)^2 + 4\gamma_{\mathrm{off}}\gamma_{\mathrm{on}}}]/(2\gamma_{\mathrm{off}})\}$. Thus, the corresponding $\mathbb{P}_{st}(\theta)$ also has only one maximum for constant μ_0 because minima of a potential and maxima of its stationary distribution generally coincide when noise is additive (Fig. S4 in [10]). Since an invertible coordinate transformation never changes the number of deterministic stationary states, this result clearly indicates that the nonlinear transformation $Z = e^{\theta}/(1 + e^{\theta})$ from θ to Z is fundamental to the generation of NISB.

From the information-theoretical viewpoint, this result also shows that the dynamics of Eq. (1) to decode information on x_t as $Z(t)$ from $S(t)$ is reduced to a random walk in potential $V_f(\theta)$ with bias $\mu(t)$. The temporal integration by the random walk in the θ coordinate additively amplifies the information on x_t represented by μ_t, whereas it suppresses the noise represented by dW_t, leading to the efficient decoding of x_t from $S_g(t)$. Moreover, the potential $V_f(\theta)$ endows the dynamics with the forgetting property that enables fast tracking of changing x_t. These facts reveal that the θ coordinate is more essential than the Z coordinate for the information-decoding function of Eq. (2) in the sense that its underlying principle is described the most simply. This dynamics is represented as Eq. (2) in the Z coordinate where Z is more directly related with x_t as its posterior probability. Thus, the connection between the decoding function and NISB can be understood as a dualistic relation between the natural expression of the decoding function in the θ coordinate and the emergence of NISB in the Z coordinate. This relation may be employed to further clarify the essence of the connection between NISB and information decoding.

The decoding dynamics in the θ coordinate as a random walk also indicates the disadvantage of NISB such that it cannot memorize or reinforce the state of the system without input as deterministic SB can. In this sense, the functions of deterministic and NISBs are mutually complementary, and a transition from NISB to deterministic SB may be important to constitute an entire cellular decision-making process, in which a decision is made based on a noisy signal and the determined decision is subsequently fixed. This observation suggests that an integrated theory for both SBs will be crucial to understand various cellular information processes with noise.

Finally, the connection between NISB and the information-decoding function revealed in this work may also lead to the elucidation of the energy cost of cellular information processing because NISB is related to the extent of the nonequilibrium state, which requires the flow of free energy [13]. As recently demonstrated, information can be converted into free energy and vice versa [14], but the amount of energy required for information processing is still unclear. Because the energy cost is the common currency for coordinating the intracellular functions in a cell, the result of this study together with other recent advancements may lead to a more comprehensive understanding of the total optimality of cellular functions.

I thank Atsushi Kamimura, Yuzuru Sato, Yoshihiro Morishita, and Ryo Yokota for fruitful discussions. This work was supported by the JST PRESTO program.

*Also at PREST, Japan Science and Technology Agency (JST), 4-1-8 Honcho Kawaguchi, Saitama 332-0012, Japan.
tetsuya@mail.crmind.net; http://research.crmind.net/

[1] S. Paliwal, P. A. Iglesias, K. Campbell, Z. Hilioti, A. Groisman, and A. Levchenko, Nature (London) **446**, 46 (2007); A. Singh, Curr. Opin. Microbiol. **12**, 460 (2009); N. Ingolia and A. Murray, Curr. Biol. **17**, 668 (2007); R. Losick and C. Desplan, Science **320**, 65 (2008); K. L. Ho and H. A. Harrington, PLoS Comput. Biol. **6**, e1000956 (2010); E. Z. Bagci, Y. Vodovotz, T. R. Billiar, G. B. Ermentrout, and I. Bahar, Biophys. J. **90**, 1546 (2006).

[2] W. Horsthemke and R. Lefever, *Noise-Induced Transitions* (Springer-Verlag, Berlin, 2006), 2nd ed.

[3] Y. Togashi and K. Kaneko, Physica (Amsterdam) **205D**, 87 (2005); J. Ohkubo, N. Shnerb, and D. a. Kessler, J. Phys. Soc. Jpn. **77**, 044002 (2008).

[4] M. Samoilov and A. Arkin, Nat. Biotechnol. **24**, 1235 (2006).

[5] L. M. Bishop and H. Qian, Biophys. J. **98**, 1 (2010).

[6] M. N. Artyomov, J. Das, M. Kardar, and A. K. Chakraborty, Proc. Natl. Acad. Sci. U.S.A. **104**, 18 958 (2007).

[7] S. J. Altschuler, S. B. Angenent, Y. Wang, and L. F. Wu, Nature (London) **454**, 886 (2008).

[8] M. Acar, A. Becskei, and A. von Oudenaarden, Nature (London) **435**, 228 (2005); Y. Toyooka, D. Shimosato, K. Murakami, K. Takahashi, and H. Niwa, Development (Cambridge, U.K.) **135**, 909 (2008).

[9] T. J. Kobayashi, Phys. Rev. Lett. **104**, 228104 (2010); T. J. Kobayashi and A. Kamimura (to be published).

[10] See supplemental material at http://link.aps.org/supplemental/10.1103/PhysRevLett.106.228101 for derivations of equations and further discussion.

[11] M. N. Artyomov, M. Mathur, M. S. Samoilov, and A. K. Chakraborty, J. Chem. Phys. **131**, 195103 (2009); H. Qian, P. Shi, and J. Xing, Phys. Chem. Chem. Phys. **11**, 4861 (2009).

[12] A. Kimura and S. Onami, Dev. Cell **8**, 765 (2005).

[13] H. Qian and T. Reluga, Phys. Rev. Lett. **94**, 028101 (2005); H. Qian, Annu. Rev. Phys. Chem. **58**, 113 (2007); C. a. Miller and D. a. Beard, Biophys. J. **95**, 2183 (2008).

[14] T. Sagawa and M. Ueda, Phys. Rev. Lett. **102**, 250602 (2009); **104**, 090602 (2010); S. Toyabe, T. Sagawa, M. Ueda, E. Muneyuki, and M. Sano, Nature Phys. **6**, 988 (2010).